Analyst

Accepted Manuscript

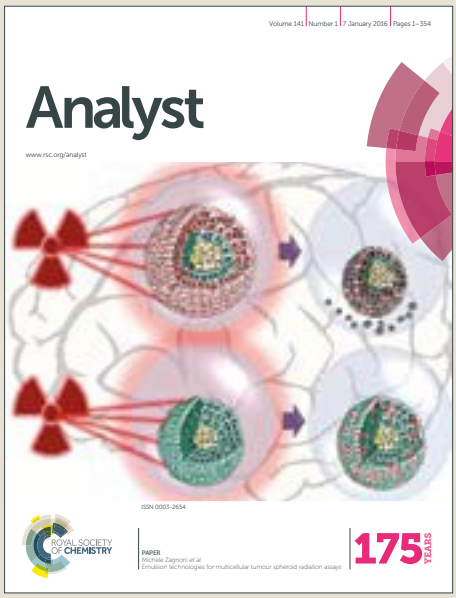

ROYAL SOCIETY OF CHEMISTRY

rsc.li/analyst

View Article Online
DOI: 10.1039/C8AN00716K

Base Excision Repair Initiated Rolling Circle Amplification-based Fluorescent Assay for Screening Uracil-DNA Glycosylase Activity Using Endo IV-assisted Cleavage of AP Probes

Jingfeng Wang[a], Yu Wang[a], Su Liu[b], Haiwang Wang[a], Xue Zhang[a], Xiaolei Song[b], Jiadong Huang[a c*]

a College of Biological Sciences and Technology, University of Jinan, Jinan 250022, P.R. China.

b College of Resources and Environment, University of Jinan, Jinan 250022, P.R. China.

c Key Laboratory of Chemical Sensing & Analysis in Universities of Shandong, college of Chemistry and Chemical Engineering, University of Jinan, Jinan 250022, P.R. China.

[*] Corresponding author. E-mail: chm_huangjd@ujn.edu.cn; Tel.: +86-531-89736122; Fax: +86-531- 82769122.

View Article Online
DOI: 10.1039/C8AN00716K

Abstract

Uracil-DNA glycosylase (UDG) is a greatly crucial damage repair enzyme that initiates the cellular base excision repair pathway maintaining the integrity of the genome. The abnormal UDG activity may induce the malfunction of uracil excision repair that is directly relevant with diverse diseases including cancers, genotypic disease, and human immunodeficiencys. In this work, a simple, robust and cost effective biosensing platform for ultrasensitive detection of UDG activity is established based on the combination of base excision repair-initiated primer generation for rolling circular amplification (RCA) with Endo IV-assisted signal amplification. In the presence of target UDG, UDG can catalyze the removal of uracil on hairpin probe (HP) leaving an apurinic/apyrimidinic (AP site) which can be cleaved by Endo IV and generating a primer for triggering the RCA reaction. Subsequently, numerous AP site-embedded signal probes namely as fluorescent-quenched probes combine with the RCA products to perform signal transduction and the quadradic signal amplification through Endo IV-catalyzed cleavage reaction, thus significantly enhanced fluorescent signal can be achieved for UDG activity screening. Under optimal conditions, this biosensor exhibits improved sensitivity toward target UDG with a detection limits of as low as 9.3×10^{-5} $U\cdot mL^{-1}$ and a widened detection range of 5 orders of magnitude. Additionally, our biosensor demonstrates high selectivity toward UDG and owns the superiority of simplicity, rapidness, and low-cost detections. Furthermore, by redesigning the modification of HP and using of the suitable endonuclease enzymes, this RCA coupled with Endo IV-assisted signal amplification strategy might be applied for the detection of other various targets, such as thymine DNA glycosylase, 8-oxoguanine DNA glycosylase,

View Article Online
DOI: 10.1039/C8AN00716K

DNA methyltransferase, and so on. Hence, the proposed strategy indeed provides a useful and versatile biosensing platform for ultrasensitive detection of UDG activity and related fundamental biomedicine research and clinical diagnosis.

Keywords: UDG detection, rolling circular amplification, Endo-assisted signal amplification, fluorescent-quenched probes

View Article Online
DOI: 10.1039/C8AN00716K

Introduction

It is one of the most common modalities of DNA hydrolytic damage that frequently deamination of cytosine to generate uracil (U), which results in the exchange of a G:C base pair to a A:U (A:T) base pair during DNA replication that disturbs genome integrity [1]. Uracil-DNA glycosylase (UDG) is a highly conserved damage repair enzyme that starts the base excision repair (BER) pathway by catalyzing the cleavage the N-glycosidic bond between the uracil base and the sugar of the nucleotide, releasing the damaged base and producing an abasic site (AP site). The BER pathway is finished through the coordinating work of additional enzymes that used for removing AP site from the duplex and subsequently replacing it by the correct cytosine base [2-5]. It is notable that abnormal UDG activity may induce the malfunction of uracil excision repair that is directly relevant with diverse diseases including cancers, genotypic disease, and human immunodeficiency [6-8]. Therefore, the high sensitive and selective detection of UDG activity is of great significance for fundamental biomedicine research and related clinical diagnosis.

The classically used strategies for UDG activity mainly involve gel electrophoresis, mass spectrometry, and radioactive labeling [9-11]. However, these methods usually suffer from labor-consuming procedures, complicated equipments, hazardous radiation, and poor sensitivity. Alternatively, some new biosensing techniques such as electrochemical [12-14], colorimetric [15, 16], and fluorescent methods [17, 18] have been developed for simple, efficient, and low-cost sensing of UDG activity with high sensitivity and specificity. But electrochemical-based strategies maybe not be appropriate for the widespread application because of the shortcomings of fussy electrode treatment steps, long reaction time on interface, and non-ideal

View Article Online
DOI: 10.1039/C8AN00716K

reproducibility. Colorimetric methods offer the advantages of simplicity, and cost efficiency, however, low sensitivity restricts its utility likewise for routine assay. Fluorescent methods, relatively speaking, are generally recognized as the perfect candidates due to their rapidness, accuracy, high-efficiency, and high detection sensitivity. Current fluorescent strategies for screening UDG activity are primary divided into two categories: label-free assay and labeled assay. In the label-free fluorescent assays, some fluorophores like SYBR Green I, N-methyl-mesoporphyrin IX (NMM) and Thioflavin T (ThT) are employed in constructing label-free fluorescent biosensor for monitoring the activity of UDG [19-21]. Although these fluorophores-based sensing strategies have cost superiority without the need of labeled probe, they maybe encounter background signal originating from non-specific absorption between fluorophores and nucleic acid probes. Alternatively, the use of the double labeled fluorescent probe that both the fluorophore such as FAM, Cy3, or Cy5, and the quencher such as Dabcyl, or BHQ are employed to modify the probe, could effectively avoid the false-positive problem generated by non-specific interaction, endowing the high specificity of labeled assay [22, 23]. To further improve the sensitivity of the fluorescent assays, isothermal nucleic acid amplification strategies, such as nicking endonuclease-assisted signal amplification (NESA) [24-28], DNAzyme [29-32], or RNase H-based signal amplification [33, 34], have been exploited for highly sensitive detection of UDG activity. However, these methods need either two or more than two kinds of tool enzymes or RNA substrates that could be easy for degradation by ubiquitous RNase H, generating high reagent expenditure or meticulous operation. Therefore, there is still a huge demand for developing simple, robust, and low-cost fluorescent methods for screening UDG activity with high sensitivity and specificity.

View Article Online
DOI: 10.1039/C8AN00716K

Herein, we construct a simple, rapid, and cost effective biosensing platform for ultrasensitive detection of UDG activity by the combination of base excision repair-initiated primer generation for RCA with Endo IV-assisted signal amplification. In our designed strategy, there are several aspects that make sense as follows. Firstly, a hairpin probe containing one uracil base and primer sequence used for activating rolling circle amplification (RCA) reaction is indigenous designed. By utilizing of base excision repair ability of target UDG coupled with endonuclease IV (Endo IV)-catalyzed cleavage of AP site, RCA primer can be controllably released, aiming to achieve target-triggered RCA amplification. Moreover, improved detection sensitivity may be acquired owing to its high amplification efficiency and rapid amplification kinetics typically providing an approximately 1000-fold to 10000-fold increase for linear amplification [35-38]. Secondly, we design an AP site-embedded dually-labeled fluorescent probe (AP probe), which is used to perform signal transduction and participate in Endo IV-catalyzed signal amplification. Because Endo IV-catalyzed cleavage of fluorescent probe is induced by UDG-triggered excision repairing of uracil in hairpin probe, fluorescent signal acquired is totally generated by specific interaction between target and DNA substrate, rather than other non-specific factors. Additionally, the use of dually-labeled fluorescent probe also affords high signal to noise ratio. Thirdly, except for RCA amplification, Endo IV-assisted cyclic cleavage reaction is incorporated to further improve the detection sensitivity. This RCA coupled with Endo IV-aided signal amplification strategy enables ultrasensitive detection of UDG activity with a detection limit of as low as 9.3×10^{-5} U·mL^{-1}. On the basis of the above significant aspects, our base excision repair-initiated RCA coupled with Endo IV-assisted signal amplification strategy may construct a simple, robust,

View Article Online
DOI: 10.1039/C8AN00716K

and cost effective biosensing platform for ultrasensitive detection of UDG activity and related fundamental biomedicine research and clinical diagnosis.

2. Experimental section

2.1 Materials and Reagents

All sequences of which oligonucleotides listed in **Table 1**were HPLC-purified and synthesized by Sangon Biotechnology Co. Ltd. (Shanghai, China). *E.coli* uracil DNA glycosylase (UDG), endonuclease IV (Endo IV), T4 DNA ligase, 10×T4 DNA ligase reaction buffer (50 mM Tris-HCl, 10 mM $MgCl_2$, 10 mM DTT, 1 mM ATP, pH 7.5), *E.coli* exonuclease I (Exo I), *E.coli* exonuclease III (Exo III), phi29 DNA polymerse, 10×phi29 DNA polymerse reaction buffer (50 mM Tris-HCl, 10 mM $MgCl_2$, 10 mM $(NH_4)_2SO_4$, 4 mM DTT, pH 7.5), deoxynucleotide (dNTP) solution mix, uracil glycosylase inhibitor (UGI), 8-oxoguanine DNA glycosylase (hOGG1), human alkyl adenine DNA glycosylase (hAAG), bovine serum albumin (BSA) were purchased from New England Biolabs (Ipswich, MA, USA). Thymine DNA glycosylase (TDG) was bought from R&D System (Minneapolis, Minnesota, USA). The agarose and DNA marker (DL15000) were purchased from Takara Biotechnology Co. Ltd. (Dalian, China). Thermo Scientific O'Range Ruler 10 bp DNA Ladder (10-150 bp) was purchased from Thermo Fisher Scientific Co. Ltd. (MA, USA). Other chemicals were of analytical grade and were used without further purification. Ultrapure water obtained from a Millipore filtration system was used throughout.

Table 1. DNA oligonucleotides sequence used in this work

Oligonucleotide name	Sequence (5' to 3')
hairpin probe (HP)	GTGATACTGATT**TCAGGCCGTCAG**UATCAC
linear padlock probe	P-CTGAGCTACGTAGTATCAGATAGATCTGTCAAG TCTGATAGTAGTATCAGATAGATCTGACGGC

View Article Online
DOI: 10.1039/C8AN00716K

ligation probe	CGTAGCTCAGGCCGTCAG
fluorescent-quenched probe (AP probe)	GTAGTAT(FAM)CAXAT(Dabcyl)AGATCTG-C3 Spacer

The region of the U base in hairpin probe (HP) is highlighted in red, which indicates the uracil deoxyribonucleotide modification, and the part in bold is the complementary sequences to the circular template. The P in the linear padlock probe denotes a 5' phosphate modification, and the underlined regions signify the binding region with the ligation probe. The fluorescent-quenched probe (AP probe) is labeled with fluorescein isothiocyanate (FAM) fluorophore and 4-(4-dimethylaminophenyl) diazinylbenzoic acid (Dabcyl) quencher, and the X highlighted in red is the tetrahydrofuran abasic site mimic (AP site), the C3 spacer modified at 3' end is used to prevent exonuclease and polymerase to play a role.

2.2 Apparatus

Gel electrophoresis was conducted using DYCZ-24DN electrophoresis cell (LIUYI, Beijing, China) and Bio-Rad Gel imaging system (Bio-Rad, USA). Fluorescence spectra were recorded using an Agilent Cary Eclipse spectrofluorometer (Agilent, USA) with excitation at 486 nm. The slit was set to be 5 nm for both the excitation and the emission.

2.3 Preparation of Circular Template

The circular template was prepared via an intramolecular ligation in an aliquot of 60 μL reaction system containing 6 μL of 100 nM 5'-phosphorylated linear padlock probe, 6 μL of 100 nM ligation probe, 6 μL 10×T4 DNA ligase reaction buffer (50 mM Tris-HCl, 10 mM $MgCl_2$, 10 mM DTT, 1 mM ATP, pH 7.5) which were added and incubated for initial denaturation at 95 ℃ for 5 min, then slowly cooled down to

View Article Online
DOI: 10.1039/C8AN00716K

room temperature. After that, 3 μL of 20 $U \cdot \mu L^{-1}$ T4 DNA ligase was added and incubated at 16 ℃ overnight. The ligation reaction solution was terminated by a thermal treatment at 65 ℃ for 10 min to inactivate the T4 DNA ligase. Subsequently, 2 μL Exo I, 2 μL Exo III were added to the ligation reaction solution above followed by incubation 2 h at 37 ℃ to digest the free and hybridized probe. The resultant products were stored at 4 ℃ for further use after inactivating Exo I and Exo III at 80 ℃ for 20 min.

2.4 Detection of UDG Activity

The detailed procedure was as follows: 2 μL of 10 nM circular template prepared above and 2 μL of 10 nM HP were added into 20 μL of amplification reaction mixture containing 2 μL 10×phi29 DNA polymerase reaction buffer (50 mM Tris-HCl, 10 mM $MgCl_2$, 10 mM $(NH_4)_2SO_4$, 4 mM DTT, pH 7.5), 2 μL of 1 mM dNTPs, 2 μL of different concentrations of UDG, 2 μL of 1 $U \cdot \mu L^{-1}$ Endo IV, 2 μL of 1 $U \cdot \mu L^{-1}$ phi29 DNA polymerase which were incubated at 37 ℃ for 90 min for UDG excision repair-initiated rolling circle amplification. Subsequently, 2 μL of 10 μM fluorescent-quenched probe (AP probe) was added into the reaction solution for Endo IV-mediated with RCA to form dual-signal amplification assay. Ultimately, the above reaction solution was mixed with 80 μL of ultrapure water and scanned using Agilent Cary Eclipse spectrofluorometer. Unless noted otherwise, all experiments for UDG measurements were repeated three times in this research.

2.5 Characterization of Gel electrophoresis

The gel electrophoresis was performed to analyze the RCA reaction products on a 1% agarose gel and the reaction products in the presence of UDG on a 4% agarose gel with a fluorescence stain Cyber Gold (0.5 $\mu g \cdot mL^{-1}$) in 50 mM Tris-borate running

View Article Online
DOI: 10.1039/C8AN00716K

buffer (pH 8.2) containing 2 mM EDTA at 145 V for 35 min. After electrophoresis, the gel was visualized via fluorescence detection using a Bio-Rad Gel imaging system.

2.6 Evaluation of UDG activity inhibition

To evaluate the inhibition of UDG activity, we selected the different concentration uracil glycosylase inhibitor (UGI) which as a powerful biochemical tool for drugs screening to perfect experimental system. UGI can bind with UDG in 1:1 molar stoichiometry, forming UGI-UDG complexes featuring greatly tight and physiologically irreversible. Thus, 2 μL of 10 nM hairpin probe was incubated with the addition of 1 $U \cdot mL^{-1}$ UDG and various concentrations of UGI. Ultimately, the above reaction solution was mixed with 80 μL of ultrapure water and scanned using Agilent Cary Eclipse spectrofluorometer after incubating with the addition of 2 μL of 10 μM AP probe. All experiments were repeated three times.

2.7 Cell culture and cellular assay

Hela cells were cultured in Dulbecco's modified Eagle's medium (DMEM; Gibco, U.S.A) supplemented with 10% fetal bovine serum (FBS, Gibco, U.S.A) and 1% penicillin-streptomycin (Gibco, U.S.A). Hela cells were cultured in a humidified atmosphere containing 5% CO_2 at 37 ℃. Hela cells were collected with trypsinization in the exponential phase of growth and washed with PBS (pH 7.4, Gibco, U.S.A). Then Hela cells were suspended in 100 μL of lysis buffer (20 mM Tris, pH 7.5, 150 mM NaCl, 1% Triton X-100, sodium pyrophosphate, β-glycerophosphate, EDTA, Na_3VO_4, leupeptin) and then centrifuged at 12000 g for 20 min at 4 ℃. The supernatant was transferred into a fresh tube and stored at -80 ℃ for further use. For the inhibition assay, 0.1 $U \cdot mL^{-1}$ UGI was incubated with Hela cell lysis at 37 ℃ for

View Article Online
DOI: 10.1039/C8AN00716K

20 min. Ultimately, the above reaction solution was mixed with ultrapure water and scanned using Agilent Cary Eclipse spectrofluorometer.

3. Results and discussion

3.1 Principle of the proposed strategy

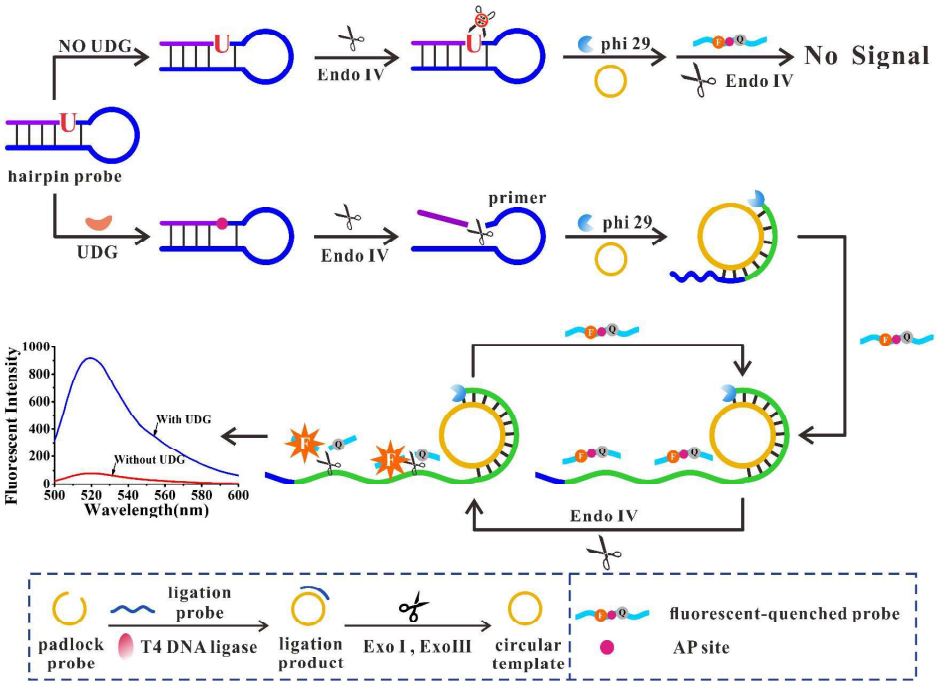

Scheme 1. Schematic diagram of the fluorescent sensing of UDG activity based on base excision repair-initiated RCA coupled with Endo IV-assisted signal amplification. U denotes the uracil deoxyribonucleotide.

Scheme 1 shows the principle of the proposed strategy for ultrasensitive detection of UDG activity. The hairpin probe (HP) is ingeniously designed to involve one uracil base in the stem region at the 3' terminus and a primer sequence used for annealing with the circular template and starting RCA reaction. A dually-labeled fluorescent probe named AP probe is mixed with a tetrahydrofuran abasic site mimic located at the middle of fluorophore (FAM) and quencher (Dabcyl), which can hybridize with the RCA products and generate the duplex DNA containing the recognition site for

View Article Online
DOI: 10.1039/C8AN00716K

Endo IV. In the presence of UDG, UDG specifically recognizes uracil and catalyzes the cleavage of the N-glycosidic bond between uracil base and the deoxyribose phosphate backbone of HP, releasing the uracil and generating an apyrimidinic site. Because Endo IV can degrade the apurinic/apyrimidinic site within the double-stranded DNA, the resultant AP site is cleaved, thus HP is divided into two splits. The purple fragment can be dissociative from the HP due to the very melting temperature (Tm ~ -7.6 ℃). Then the cleaved HP binds to the circular template and functions as the primer to initiate RCA reaction with the help of phi29 polymerase and dNTPs, yielding a very long ssDNA that contains tandem repeated DNA segments that can anneal with the AP probes. Followed by the addition of AP probes and Endo IV, the duplex DNA containing the AP sites is generated, which is nicked by Endo IV and dissociative from the RCA product owing to the unstable interaction between the split segments and the RCA product. Subsequently, the free RCA product again combines to other AP probes, initiating new cycles of Endo IV-aided cleavage reaction. Thus, large amounts of AP probes are cleaved into two short segments, resulting in the remote distance between fluorophore and quencher, thus significantly enhanced fluorescent signal is released. In contrast, in the absence of UDG, the base excision repair process is well-inhibited. Accordingly, the succedent amplification reaction would not occur, thus no fluorescent signal is released. Therefore, our proposed strategy holds the potential of creating a simple, rapid, low-cost biosensing platform for detecting UDG activity with high sensitivity and specificity.

3.2 Feasibility of the proposed strategy in UDG activity assay

View Article Online
DOI: 10.1039/C8AN00716K

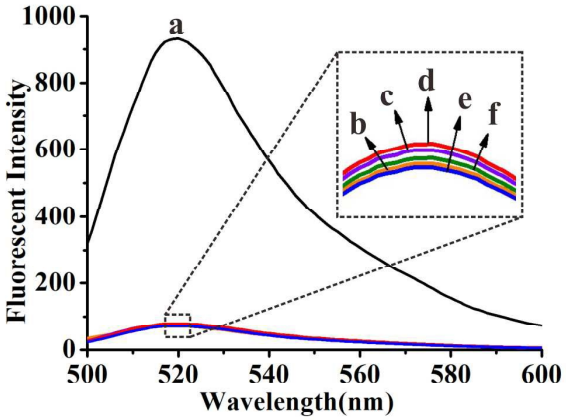

Fig. 1 Fluorescence emission spectra responses of this biosensor obtained upon analyzing 1 $U \cdot mL^{-1}$ UDG (a). Curves b to g is for the feasibility research of the strategy which is controlled with no UDG (b), no phi 29 (c), no circular template (d), non-target enzyme TDG in place of UDG (e), and normal HP (U replaced by T) in place of HP (f).

In order to investigate the viability of our proposed strategy, fluorescence emission spectra responses to a series of control experiments were obtained, and the results were shown in **Fig. 1**. In the presence of 1 $U \cdot mL^{-1}$ UDG, there is a significantly strong peak at 520 nm approximately, indicating target-initiated RCA reaction and Endo IV-catalyzed cleavage of AP probe is successfully performed, thus a substantial number of AP probes are nicked, generating remarkably enhanced fluorescent signal (curve a). In contrast, it was found that a negligible signal was acquired for blank sample, which implied base excision repair process is inhibited that subsequent amplification reaction could not occur (curve b). This suggested the liberated fluorescent signal was generated by specific interaction between UDG and substrate DNA. Additionally, the fluorescence response almost approximate to that of the blank sample was obtained in the absence of circular template (curve c) or phi 29 (curve d). This indicated single-stranded AP probes couldn't be nicked by Endo IV

View Article Online
DOI: 10.1039/C8AN00716K

due to its specificity to AP site-inseted duplex DNA. When non-target damage repair enzyme TDG in place of UDG, we observed a very weak fluorescent signal, confirming the high specificity of the method (curve e). Furthermore, a normal HP that uracil was replaced by thymine in the stem region, was introduced to verify the substrate specificity of UDG (curve f). It was observed that an invisible fluorescence peak appeared in the curves, revealing UDG was a highly conserved damage repair enzyme that specifically recognized the uracil base. The above results fully suggested the proposed strategy could be used for high specific detection of UDG.

3.3 Gel electrophoresis characterization

To further verify the feasibility of UDG-catalyzed base excision repair reaction, straightforward proof could be reflected by gel electrophoresis experiment. The results were depicted in **Fig. S1A**. Lane 1 denoted DNA marker (10-150 bp). Lane 2 displayed a bright band of our designed HP on the image. After incubation of HP with Endo IV, the brightness of the band at the position of HP was similar to that of lane 2 (lane 3). However, after incubation of HP, Endo IV with UDG, a new band was observed (lane 4). This revealed UDG removed the uracil base, generating the AP site that was nicked by Endo IV, thus two split segments were liberated. On the basis of these experiment results, it was legitimately concluded that our designed strategy should be feasible for UDG activity assay. In addition, the ligase reaction and RCA reaction were also verified by gel electrophoresis experiment, and the results were shown in **Fig. S1B.** Lane 1 was on behalf of DNA marker (15000 bp). It was observed that a bright band appeared on the image after the incubation of padlock probe and the ligation probe with T4 DNA ligase (lane 2). Similarly, a bright band with the same mobility and intensity were obtained after the incubation of padlock probe, the

View Article Online
DOI: 10.1039/C8AN00716K

ligation probe, T4 DNA ligase with Exo I and Exo III (lane 3). This represented the circular template was successfully synthesized. In contrast, no band appeared on the image after incubation the padlock probe, the ligation probe without T4 DNA ligase, illustrating the probes were digested by Exo I and Exo III (lane 4). It was reasonably concluded the circular template was commendably prepared with the aid of T4 DNA ligase, Exo I and Exo III. As seen from lane 5, a bright band with the large-molecule-weight product was present to the image. This signified RCA reaction was favourably carried out and very long ssDNA that contained tandem repeated DNA segments were achievable.

3.4 Optimization of experimental conditions

To achieve the optimal analytical performance of the biosensor, some experimental conditions including the concentration of HP, the amounts of Endo IV, and the RCA reaction time were successively investigated by fluorescence spectroscopy, and the results were shown in Fig. S2. Typically, the concentration of HP had an effect on the specific interaction between target UDG and substrate. As shown in **Fig. S2A**, it was found that the $(F_1-F_0)/F_0$ value gradually increased with increasing of HP concentration and reached equilibrium when the concentration was 10 nM. So, 10 nm was chosen as the optimal HP concentration. In addition, the amounts of Endo IV would affect cleavage efficiency of the AP probe. As shown in **Fig. S2B**, the maximum $(F_1-F_0)/F_0$ value was acquired when the concentration of Endo IV reached 1 $U \cdot \mu L^{-1}$. Thereby, 1 $U \cdot \mu L^{-1}$ was used as the optimal concentration in the subsequent experiments. Furthermore, the signal to noise ratio was also influenced by the concentration of AP probe. **Fig. S2C** depicted the maximum value was obtained at the concentration of 10 μM. Thus, we chose 10 μM as the optimized

View Article Online
DOI: 10.1039/C8AN00716K

concentration. Ultimately, the RCA-based amplification efficiency was extremely depended on the reaction time. As shown in **Fig. S2D**, the $(F_1-F_0)/F_0$ value increased with the increasing of the reaction time until a plateau was reached at 90 min. The $(F_1-F_0)/F_0$ value was changed tardily with the elapse of the reaction time. Therefore, 90 min was chosen as the optimal reaction time in the following experiments.

3.5 Analytical performance of the biosensor

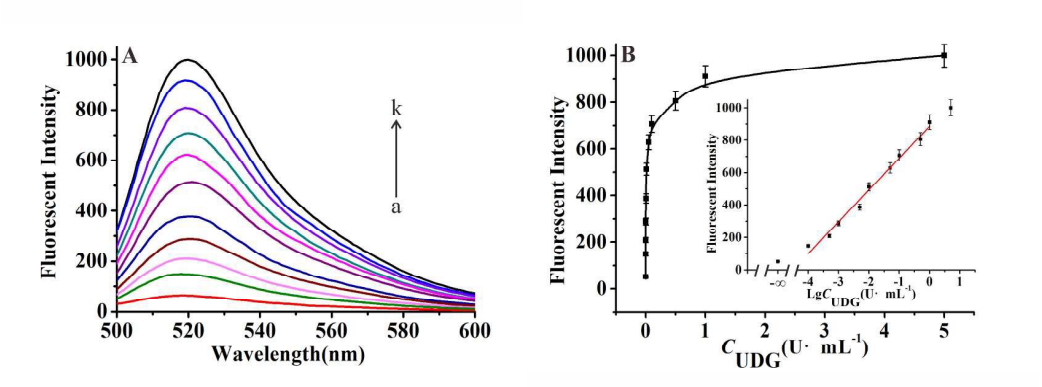

Fig. 2 (A) Fluorescent responses to the different concentrations of UDG (from curve a to k: 0, 1×10^{-4}, 5×10^{-4}, 1×10^{-3}, 5×10^{-3}, 1×10^{-2}, 5×10^{-2}, 1×10^{-1}, 5×10^{-1}, 1, 5 U·mL^{-1}). (B) The calibration curve of fluorescent intensity at 520 nm for different UDG concentrations. Error bars are standard deviations across three repetitive experiments. Inset is the plot of the fluorescent intensity at 520 nm versus the logarithm value of UDG concentration.

To demonstrate the analytical performance of the UDG activity assay, we investigated the UDG activity at various concentrations under the optimal experimental conditions by fluorescence spectroscopy. As shown in **Fig. 2A**, the normalized fluorescent intensities increased significantly with the increasing concentration range of UDG from 1×10^{-4} U·mL^{-1} to 5 U·mL^{-1} which was over 5 orders of magnitude. **Fig. 2B** displayed a linear dependence between the fluorescence

View Article Online
DOI: 10.1039/C8AN00716K

intensity at 520 nm and the logarithm of UDG concentration. The linear correlation equation is $F=885.1+196.0\times lgC_{UDG}\,(U\cdot mL^{-1})$ with a correlation coefficient of 0.9860. The detection limit was calculated to be 9.3×10^{-5} $U\cdot mL^{-1}$ in terms of the rule of 3 times standard deviation over the blank response. Additionally, the analytical performance of this biosensor for quantitative assay of UDG was compared to the earlier reported method, and the results were shown in **Table S1**. It was clearly exhibited that the sensitivity of the proposed biosensor was superior to the majority of existing methods for UDG activity detection. Moreover, our biosensor offered the advantages of shortened detection time, simplified operation, and reduced analysis cost. Hence, the developed RCA coupled with Endo IV-assisted signal amplification strategy might provide a useful and practical platform for UDG quantification.

3.6 Validation of specificity

The specificity is a crucial factor to assess the utility of the biosensor in the detection of real samples. We also evaluated the selectivity of the biosensor for monitoring the UDG activity by replacing UDG by non-target enzymes including BSA, hAAG, hOGG1, TDG. As shown in **Fig. 3**, the biosensor only showed a significantly strong fluorescence signal in the presence of target UDG, while the fluorescent response to non-target enzymes were on the verge of that of blank sample. These results distinctly demonstrated our developed strategy had admirable specificity for UDG detection.

View Article Online
DOI: 10.1039/C8AN00716K

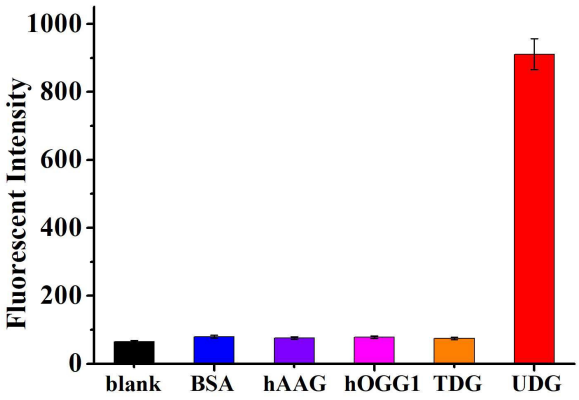

Fig. 3 Plot of the fluorescence intensities at 520 nm obtained upon different enzymes. The concentration of UDG is 1 U · mL^{-1}. The concentration of the non-target enzyme is 50 U · mL^{-1}. Error bars are standard deviations across three repetitive experiments.

3.7 UDG kinetics assay

The enzyme kinetic parameters of UDG was evaluated by monitoring the initial velocity with different concentrations of DNA substrates (HP) in 20 min of UDG-initiated uracil-excision repair reaction at 37 ℃ (UDG concentration was 10 U·mL^{-1}). As shown in **Fig. S3**, the initial velocity increased correspondingly with the increasing concentrations of HP. The kinetics parameters were calculated based on the fitting of initial velocity to the Michaelis-Menten equation $V= V_{max}[S]/ (K_m + [S])$, where V_{max} was the maximum initial velocity, [S] was the concentration of DNA substrate (HP), and K_m was the Michaelis-Menten constant. The V_{max} of UDG was evaluated to be 29.95 min^{-1} and Km was calculated to be 60.64 nM, consistent with that obtained by gel-based method[39]. These results demonstrated that our strategy could be applied for evaluating the kinetic parameters of UDG.

3.8 UDG inhibition assay

The screening of UDG inhibitor is of great importance for cancer therapies. Here, UGI was chosen as a model inhibitor to evaluate the inhibitor screening ability of our

View Article Online
DOI: 10.1039/C8AN00716K

proposed biosensor. It has been reported that UGI can bind to UDG in 1:1 stoichiometry, forming a tight and irreversible complex. As shown in **Fig. 4A**, the normalized fluorescent intensities at 520 nm weakened significantly with increasing concentration of UGI from 1 $U \cdot mL^{-1}$ to 25 $U \cdot mL^{-1}$. It was observed from **Fig. 4B** that UGI inhibited UDG in a dose-dependent manner, where UDG activity declined with increasing concentrations of UGI. All above results suggested the inhibition assay provided a potential sensing platform for monitoring UDG inhibitors and the further research of the interaction between UDG and its inhibitor.

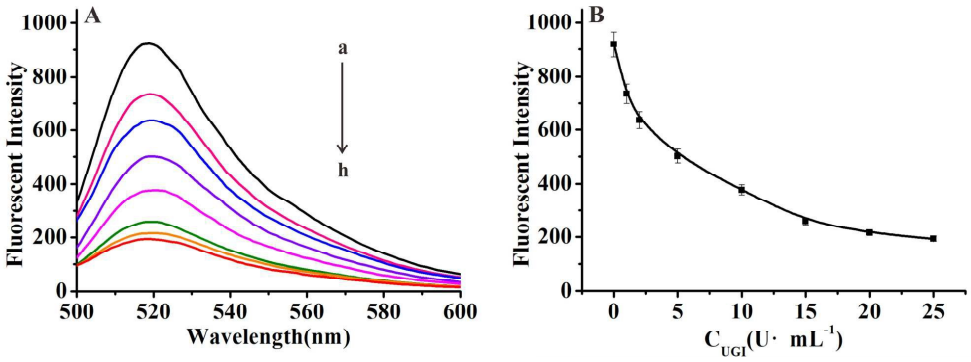

Fig. 4 (A) Fluorescent responses to the different concentrations of UGI (from curve a to h: 0, 1,2, 5, 10, 15, 20, 25 $U \cdot mL^{-1}$). The concentration of UDG is 1 $U \cdot mL^{-1}$. (B) The calibration curve of fluorescent intensity at 520 nm for different UGI concentrations. Error bars are standard deviations across three repetitive experiments.

3.9 Cellular UDG assay

To demonstrate the feasibility of the proposed strategy for cellular UDG assay, the UDG activity in Hela cells lysate was monitored, and the results were shown in **Fig. 5A**. It was observed that the biosensor showed a significantly strong fluorescent signal in the presence of Hela cells (blue column), while the fluorescent responses to the lysis buffer (black column), and the lysis buffer + UGI (red column) were on the

View Article Online
DOI: 10.1039/C8AN00716K

verge of that of blank sample. Additionally, we added UGI to inhibit the UDG activity to further confirm the fluorescence enhancement was induced by UDG rather than any other components in Hela cell. By contrast, the addition of UGI reduced the fluorescent intensity by about 60.4% (green column). **Fig. 5B** shows that the calibration curve of fluorescent intensity versus the logarithm value of cell number in the range from 5 to 10000 cells. The correlation equation is $F=130.57 \log_{10}N-4.468$ with a correlation coefficient of 0.9964, where F is the fluorescent intensity, and N is the number of Hela cells, respectively. The above results clearly demonstrated that our proposed strategy could be applied for detecting UDG activity in complicated biological matrix.

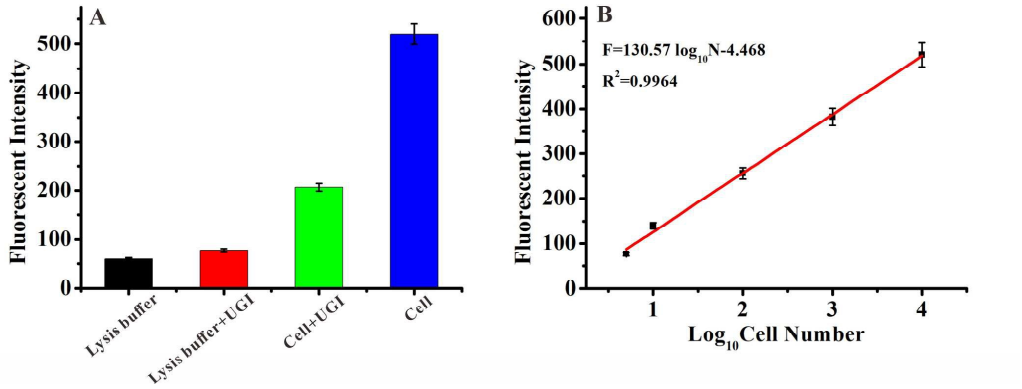

Fig. 5 (A) Scanning of fluorescent intensities in the presence of lysis buffer (black column), lysis buffer + UGI (red column), cell + UGI (green column) and cell (blue column) respectively. (B) The calibration curve of fluorescent intensity at 520 nm versus the logarithm value of cell number. Error bars are standard deviations across three repetitive experiments.

4. Conclusions

In this work, a simple, rapid, and cost-effective fluorescence assay for ultrasensitive detection of UDG activity has been developed using target

View Article Online
DOI: 10.1039/C8AN00716K

UDG-initiated RCA coupled with Endo IV-assisted signal amplification. Our strategy relies on base excision repair-mediated AP site generation and subsequent cleavage of AP site via Endo IV, which induces RCA reaction and Endo IV-catalyzed cyclic cleavage of AP probes. Owing to the preponderances that high amplification efficiency and rapid amplification kinetics of this amplification strategy, this developed biosensor can specifically monitor UDG activity with a detection limit of as low as 9.3×10^{-5} U · mL^{-1} and a detection range of 5 orders of magnitude. In addition, we employ the inhibition assay of UDG to construct a potential sensing platform for monitoring UDG inhibitors and the further research of the interaction between UDG and its inhibitor. Furthermore, this RCA coupled with Endo IV-assisted signal amplification strategy could be applied for the detection of other widespread targets (e.g. thymine DNA glycosylase, 8-oxoguanine DNA glycosylase, and DNA methyltransferase) by redesigning the modification of substrate DNA and using of the suitable endonuclease enzymes. Therefore, the developed biosensor may create a useful and versatile platform for ultrasensitive screening of UDG activity and related fundamental biomedicine research and clinical diagnosis.

Acknowledgements

This work was supported by National Natural Science Foundation of China (31471644), the Primary Research & Development Plan of Shandong Province (2017GSF220009, 2016GSF120006) and the Natural Science Foundation of Shandong Province of China (ZR2016BL27).

References

1. Q. Jin, A. M. Fleming, R. P. Johnson, Y. Ding, C. J. Burrows and H. S. White, J. Am. Chem. Soc., 2013, 135, 19347-19353.

View Article Online
DOI: 10.1039/C8AN00716K

2. N. Schormann, R. Ricciardi and D. Chattopadhyay, Protein Sci., 2014, 23, 1667-1685.
3. G. Slupphaug, C. D. Mol, B. Kavli, A. S. Arvai, H. E. Krokan and J. A. Tainer, Nature, 1996, 384, 87-92.
4. T. Lindahl, Proceedings of the National Academy of Sciences of the United States of America, 1974, 71, 3649-3653.
5. S. S. Parikh, C. D. Mol, G. Slupphaug, S. Bharati, H. E. Krokan and J. A. Tainer, The EMBO journal, 1998, 17, 5214-5226.
6. K. Imai, G. Slupphaug, W.-I. Lee, P. Revy, S. Nonoyama, N. Catalan, L. Yel, M. Forveille, B. Kavli, H. E. Krokan, H. D. Ochs, A. Fischer and A. Durandy, Nature immunology, 2003, 4, 1023-1028.
7. J. H. Hoeijmakers, Nature, 2001, 411, 366-374.
8. T. Lindahl, Nature, 1993, 362, 709-715.
9. H. Krokan and C. U. Wittwer, Nucleic acids research, 1981, 9, 2599-2613.
10. A. A. Ischenko and M. K. Saparbaev, Nature, 2002, 415, 183-187.
11. J. Tchou, H. Kasai, S. Shibutani, M. H. Chung, J. Laval, A. P. Grollman and S. Nishimura, Proceedings of the National Academy of Sciences of the United States of America, 1991, 88, 4690-4694.
12. M. A. McWilliams, F. H. Anka, K. J. Balkus and J. D. Slinker, Biosensors & Bioelectronics, 2014, 54, 541-546.
13. X. J. Liu, M. Q. Chen, T. Hou, X. Z. Wang, S. F. Liu and F. Li, Electrochim. Acta, 2013, 113, 514-518.
14. H. Zhang, L. L. Zhang, J. H. Jiang and R. Q. Yu, Anal. Sci., 2013, 29, 193-198.
15. V. T. Nguyen, D. V. Le, C. Nie, D. M. Zhou, Y. Z. Wang, L. J. Tang, J. H. Jiang and R. Q. Yu, Talanta, 2012, 100, 303-307.
16. X. J. Liu, M. Q. Chen, T. Hou, X. Z. Wang, S. F. Liu and F. Li, Biosensors & Bioelectronics, 2014, 54, 598-602.
17. J. J. Zhao, Y. F. Ma, R. M. Kong, L. L. Zhang, W. Yang and S. L. Zhao, Anal. Chim. Acta, 2015, 887, 216-223.
18. Y. C. Du, L. N. Zhu and D. M. Kong, Biosensors & Bioelectronics, 2016, 86, 811-817.
19. C. B. Ma, K. F. Wu, H. S. Liu, K. Xia, K. M. Wang and J. Wang, Talanta, 2016, 160, 449-453.
20. X. F. Zhang, N. Li, Y. Ling, L. Tang, N. B. Li and H. Q. Luo, Sens. Actuator B-Chem., 2018, 255, 2589-2594.

View Article Online
DOI: 10.1039/C8AN00716K

21. W. F. Du, J. J. Li, F. B. Xiao, R. Q. Yu and J. H. Jiang, Anal. Chim. Acta, 2017, 991, 127-132.
22. F. Tang, X.-W. Xing, J.-M. Chu, Q. Yuan, X. Zhou, Y.-Q. Feng and B.-F. Yuan, Analyst, 2015, 140, 4636-4641.
23. X. Miao, Z. Li and L. Ling, Analyst, 2016, 141, 5829-5834.
24. X. Q. Leng, Y. Wang, S. Liu, Q. Q. Pei, X. J. Cui, Y. Q. Tu, X. J. Liu and J. D. Huang, Sens. Actuator B-Chem., 2017, 252, 689-696.
25. Y. Zhang, X. Y. Wang, Q. Y. Zhang and C. Y. Zhang, Analytical Chemistry, 2017, 89, 12408-12415.
26. B. C. Yin, Y. Q. Liu and B. C. Ye, Analytical Chemistry, 2013, 85, 11487-11493.
27. H. Wang, H. H. Wang, X. R. Duan, X. D. Wang, Y. Y. Sun and Z. P. Li, Sens. Actuator B-Chem., 2017, 252, 215-221.
28. Z. Y. Wang, F. Li, Y. Zhang, H. Zhao, H. Xu, Z. S. Wu, J. X. Lyu and Z. F. Shen, Sens. Actuator B-Chem., 2017, 251, 692-698.
29. X. Li, J. Q. Xie, B. Y. Jiang, R. Yuan and Y. Xiang, ACS Appl. Mater. Interfaces, 2017, 9, 5733-5738.
30. N. Cai, Y. Li, S. Chen and X. Su, Analyst, 2016, 141, 4456-4462.
31. D. He, L. Hai, H. Wang, R. Wu and H.-W. Li, Analyst, 2018, 143, 813-816.
32. L. Zhou, X. Shen, N. Sun, K. Wang, Y. Zhang and R. Pei, Analyst, 2015, 140, 5450-5453.
33. L. B. Wang, H. Y. Zhou, B. Liu, C. Zhao, J. L. Fan, W. Wang and C. Y. Tong, Analytical Chemistry, 2017, 89, 11014-11020.
34. L.-j. Wang, M. Ren, Q. Zhang, B. Tang and C.-y. Zhang, Analytical Chemistry, 2017, 89, 4488-4494.
35. W. Zhao, M. M. Ali, M. A. Brook and Y. Li, Angewandte Chemie (International ed. in English), 2008, 47, 6330-6337.
36. S. V. Hamidi, H. Ghourchian and G. Tavoosidana, Analyst, 2015, 140, 1502-1509.
37. X. Ou, B. Wei, Z. Zhang, M. Zhang, Y. Zhuang, P. Gao, X. Lou, F. Xia and B. Z. Tang, Analyst, 2016, 141, 4394-4399.
38. J. Song, F. Yin, X. Li, N. Dong, Y. Zhu, Y. Shao, B. Chen, W. Jiang and C.-z. Li, Analyst, 2018, 143, 1593-1598.
39. A. Maksimenko, A. A. Ishchenko, G. Sanz, J. Laval, R. H. Elder and M. K. Saparbaev, Biochemical and Biophysical Research Communications, 2004, 319, 240-246.

View Article Online
DOI: 10.1039/C8AN00716K

Title Text

Base Excision Repair Initiated Rolling Circle Amplification-based Fluorescent Assay for Screening Uracil-DNA Glycosylase Activity Using Endo IV-assisted Cleavage of AP Probes

Jingfeng Wang, Yu Wang, Su Li, Haiwang Wang, Xue Zhang, Xiaolei Song, Jiadong Huang

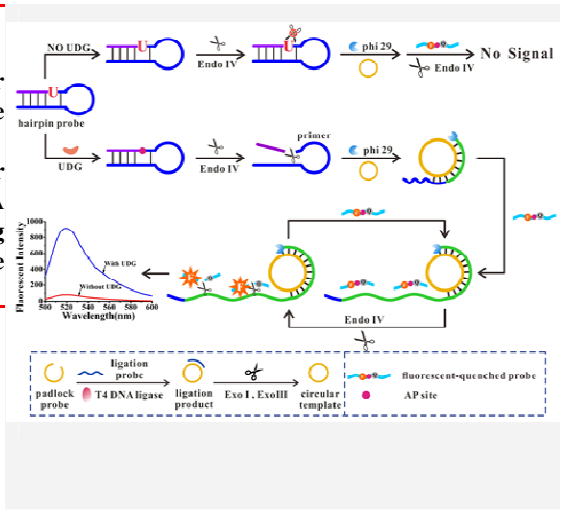

A simple, robust and cost effective biosensing platform for ultrasensitive detection of UDG activity is established based on the combination of base excision repair-initiated primer generation for rolling circular amplification (RCA) with Endo IV-assisted signal amplification.